Pinching Dynamics and Multiple Droplet Generation in Partial Coalescence

Teng Dong and Panagiota Angeli*
ThAMeS Multiphase, Department of Chemical Engineering, University College London, London WC1E 7JE, United Kingdom

(Received 1 November 2022; revised 27 January 2023; accepted 4 August 2023; published 6 September 2023)

When a drop merges with its homophase, a liquid cylinder appears in certain conditions, which is pinched off leading to partial coalescence. We investigate the process experimentally and numerically, and find that the Rayleigth-Plateau instability is able to pinch off the cylinder when its height-to-neck ratio exceeds one. Surfactants are found to attenuate the cylinder and produce multiple droplets at moderate concentrations. For both the pinch-off of the mother drop and the subsequent breakup of the liquid threads in partial coalescence, the neck thinning is initially in the inertial (I) regime and then shifts to the inertial-viscous (IV) regime. An intermediate regime is seen at larger surfactant concentrations, which accelerates the thinning and favours the generation of multiple droplets.

DOI: 10.1103/PhysRevLett.131.104001

Introduction.—Two liquid bodies tend to merge when brought into contact, to minimize their surface energy. Under certain conditions, merging is not completed but leaves a small droplet behind, resulting in partial coalescence [1], which is often observed in nature and various industrial processes [2–8]. In partial coalescence, the drop takes the shape of a liquid cylinder that pinches off to form a secondary droplet (see Fig. 1). Early researchers Charles and Mason [9] attributed the cylinder pinch-off to the Rayleigh-Plateau (RP) instability [10,11]. Recently, Blanchette and Bigioni [12] suggested that the RP instability was not the cause of partial coalescence. Other researchers reached the same conclusion by analyzing the propagation of capillary waves along the drop surface [13–15]. A consensus emerged that the pinch-off results from the competition between the horizontal and the vertical collapse of the droplet as it joins its bulk homophase. With the vertical collapse inhibited by the convergence of the capillary waves, the inward horizontal collapse is able to develop and lead to the cylinder pinch-off [12,13].

Since the liquid viscosity mainly resists the evolution of capillary waves, the Ohnesorge number, $\mathrm{Oh} = \mu_d/\sqrt{\rho_d \sigma R}$ is generally used to characterize the process, where μ_d and ρ_d are the viscosity and the density of the drop liquids, R is the drop radius, and σ is the surface tension [12,16]. Above a critical Oh number, partial coalescence is hindered, as viscosity dampens the capillary waves. This was clearly seen for the coalescence of a drop with a liquid surface in contact with air [12]. In contrast, the boundary between the partial and total coalescence at liquid-liquid interfaces is less clear compared to the cases at air-liquid surfaces [17–19]. If the capillary waves are responsible for partial coalescence, the phenomenon should be different between bubbles and drops, as the liquid viscosity dissipates the energy of capillary waves and affects the momentum in the fluids. However, Pucci *et al.* [20] found that the coalescence of bubbles was similar to that of droplets. In addition, Gilet *et al.* [19] observed partial coalescence without evident capillary waves. Furthermore, Oh cannot accurately predict the size ratio of the daughter to mother drop, which is commonly measured to indicate the extent of partial coalescence [1,21]. The complexity of partial coalescence discussed above reveals that the capillary waves may not be the only mechanism involved. In this Letter, we reestablish the crucial role of Rayleigh-Plateau instability in partial coalescence while the capillary waves are only important in the generation of the initial liquid cylinder but not the main cause. In addition, we show partial coalescence experiments that produce multiple droplets. For both the pinch-off of the mother droplet and the breakup of the subsequent liquid threads, the neck thinning is found to be similar to the breakup of liquid filaments.

Partial coalescence mechanism.—To revisit the partial coalescence dynamics, the coalescence of aqueous droplets with 33% glycerol and diameter of $D = 3.62$ mm at the interface between 0.65 cSt silicone oil and their homophase are experimentally studied. A high-speed camera is used to capture the process. Numerical simulations for the same case are conducted by solving the axisymmetric incompressible Navier-Stokes equations, using the volume of fluid (VOF) model to track the interfaces. The deformed drop surface and the interface between the two immiscible liquids before coalescence are extracted from the experiments to initialize the simulation. Validation is performed by comparing the droplet shapes between the simulations

Published by the American Physical Society under the terms of the Creative Commons Attribution 4.0 International license. Further distribution of this work must maintain attribution to the author(s) and the published article's title, journal citation, and DOI.

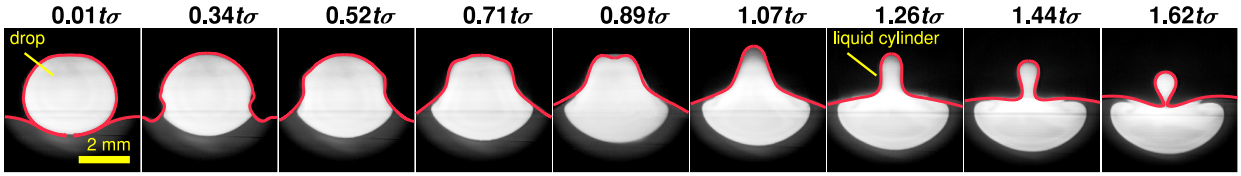

FIG. 1. Partial coalescence of a droplet of 33% glycerol at the interface between the 0.65 cSt silicone oil and its homophase. The red curves outlining the droplet are extracted from the simulations.

and the experiments, and good agreement is achieved as shown in Fig. 1.

Both experiments and simulations show that the capillary waves along the droplet surface have converged on the drop summit slightly before the generation of the liquid cylinder (see video S2 in Supplemental Material [22]). Thus, the capillary waves only help to build the initial cylinder and do not contribute to the pinch-off in the following steps. To check whether the RP instability dominates the pinch-off, we follow the procedure of Blanchette and Bigioni [12] to interrupt the normal simulation (NS) when the liquid cylinder has its maximum height at roughly $1.29t_\sigma$. The tracking is scaled with capillary time $t_\sigma = \sqrt{\rho_d R^3/\sigma}$. At this point, we set the velocity and the pressure fields to 0 and restart the simulation so that only capillary forces are relevant. The subsequent stages of the test simulation (TS1) are shown with red curves in Fig. 2. It is seen that the neck does not expand directly after the start of TS1 but continues to narrow down, though it fails eventually to pinch off; this is found as well in the case studied by Blanchette and Bigioni [12].

According to the theory [9,10], the RP instability is only able to evolve when the height of the liquid cylinder exceeds its circumference. As shown in Fig. 3(a), the height-to-circumference ratio $\psi = h/\pi w_n$ at $1.29t_\sigma$ is 0.53 that is much lower than 1. Here, w_n is the width of the cylinder neck and h is the vertical distance from the

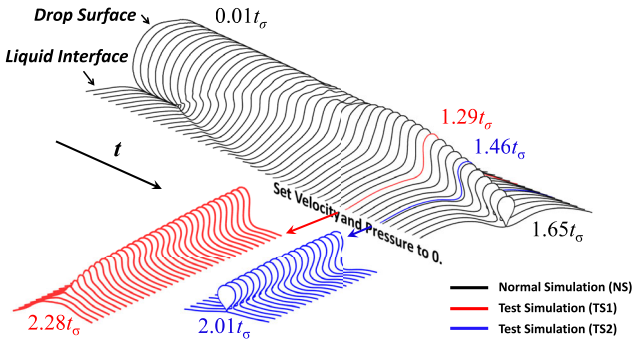

FIG. 2. Simulated drop evolution in partial coalescence. The black curves present the drop surface evolution for normal simulation (NS) starting from $0.01t_\sigma$ as shown in Fig. 1. The red and blue curves represent the test simulations by interrupting the NS and setting the velocity and pressure fields to 0 at instants $1.29t_\sigma$ (TS1) and $1.46t_\sigma$ (TS2), respectively.

cylinder top to the neck, as shown in Fig. 3(e). However, $\psi \approx 1$ at a later instant $1.46t_\sigma$, where the RP instability should be able to develop. To test this, a new test simulation (TS2) is conducted, which starts at $1.46t_\sigma$ where the velocity and pressure fields are set to 0. As the blue curves show in Fig. 2, TS2 generates a daughter droplet at $2.01t_\sigma$, which proves that the RP instability leads to the pinch-off. The Bond number in the current study is $\mathrm{Bo} = \Delta\rho g R^2/\sigma = 0.5$, while for the case of Blanchette and Bigioni [12], $\mathrm{Bo} = 0.09$. To test the influence of gravity, we repeat the numerical study by Blanchette and Bigioni [12] but interrupt the simulation at a later instant where $\psi > 1$ and find also that a daughter droplet forms, see Fig. S5 in Supplemental Material [22].

As the RP instability does not lead to the pinch-off for TS1 at $1.29t_\sigma$, but only for TS2 starting at $1.46t_\sigma$, a question remains of what drives the continuous thinning of the cylinder between these two times in the NS. According to the Young-Laplace equation, the pressure difference across the interface is $\Delta P = \sigma(\kappa_\theta + \kappa_a)$, where $\kappa_\theta = 1/R_\theta$ is the azimuthal curvature and $\kappa_a = 1/R_a$ the axial curvature [26]. As shown in Fig. 3(b), for NS at $1.29t_\sigma$, the pressure is maximum at the cylinder top in region C, as it includes the positive contribution from both the azimuthal curvature κ_θ and the axial curvature κ_a. At region B slightly above the neck, the cylinder has a flat shape with no axial curvature. The high pressure from only the azimuthal curvature tends to pinch off region B. At region A below the neck, low pressure is seen as the axial curvature changes sign from inward to outward. At $1.29t_\sigma$, the liquids at the neck have retained their high velocity from the previous stages. Because of the Bernoulli effect, the pressure decreases even more at this high-velocity area. The large pressure difference between B and A strengthens the Bernoulli effect. As shown in Fig. 3(b), this trend becomes stronger after $1.29t_\sigma$ and accelerates the drainage of the liquid from the neck. Especially at $1.47t_\sigma$ where $\psi > 1$, the pressure in region B near the neck becomes higher than that in the neighboring areas above and below; this further prevents the drainage of liquid from C to B, while it promotes the drainage from B to A until the pinch-off at $1.67t_\sigma$.

For TS1 starting at $1.29t_\sigma$, a pressure difference from C to A builds quickly at $1.31t_\sigma$ with a similar pattern to that of NS at $1.29t_\sigma$, as shown in Fig. 3(c). In this case, however, it takes longer to build a high velocity at the neck and there is no significant contribution of the Bernoulli effect. In this

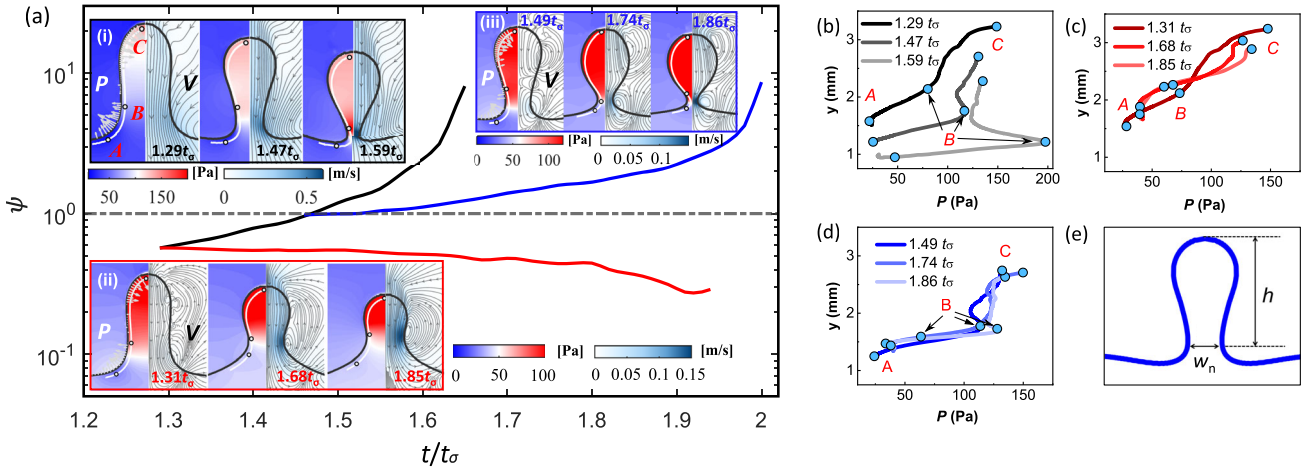

FIG. 3. (a) Evolution of the cylinder ratio ψ for NS (black), TS1 (red), and TS2 (blue). The insets (i), (ii), and (iii) illustrate the pressure (P) and the velocity (V) fields at corresponding instants. The pressures at different times along the white curves at 3 representative points A, B, and C are shown in figures (b)–(d) for NS, TS1, and TS2, respectively. White arrows are plotted along the surface with their length representing the pressure from the axial curvature κ_a in the first image of each inset group. Figure (e) indicates how h and w_n are measured.

case, the pressure difference from B to A is comparable to that from C to B in the following steps. As a result, the liquid in the whole cylinder drains, leading to a decrease of ψ that does not allow the RP instability to develop [27]. For TS2 starting at $1.46t_\sigma$, there is from the beginning a large pressure at region B due to the capillary force from the interface curvature [Fig. 3(d)]. The pressure difference between B and C prevents the liquid from the top part of the cylinder to drain while the difference between B and A promotes the liquid drainage at the neck until the pinch-off at $2.01t_\sigma$. This is clear evidence that the RP instability dominates the pinch-off after $\psi > 1$.

Multiple droplets in partial coalescence.—The breakage of liquid jets into multiple droplets under RP instability is well documented [10,28], while studies on the generation of multiple droplets during partial coalescence are limited [9,15]. Inspired by the analysis above, we generated long liquid cylinders and observed the generation of multiple droplets during partial coalescence. It was found previously that surfactants tend to thin the liquid cylinder resulting in smaller daughter droplets [18]; multiple droplets are also more likely to occur in low-viscosity systems [15]. Accordingly, a new set of experiments was conducted with water droplets coalescing at the interface between a 5 cSt silicone oil and water in the presence of oil-soluble surfactants Span 80. Mass ratios of Span 80 in oil equal to $\phi = 0$, $\phi = 1 \times 10^{-5}$ and $\phi = 2 \times 10^{-5}$ were tested.

Multiple droplets are generated from thin liquid bodies, whose shapes are largely affected by the pinching of the mother drops. To characterize this, we measure the height-to-circumference ratio $\psi = h/\pi w_b$ for the liquid body at the cylinder generation (ψ_c) and at pinch-off (ψ_p), where w_b is the width of liquid body as shown in Figs. 4(a) and 4(b). The liquid cylinder continues to thin during pinching with $\psi_p = 1.4\psi_c$, as illustrated in Fig. 4(c). Interestingly, only one droplet is generated after the liquid retraction at $\psi_p < 1$, corresponding to pure systems $\phi = 0$ and $\phi = 1 \times 10^{-5}$. For $\psi_p < 1$, type **1** is the standard partial coalescence, while type **2** is characterized by the generation of a cylinder at the bottom of the body, which recovers its spherical shape at a lower speed compared to type **1**, mainly due to the accumulation of the surfactants at the lower tip [23]. The liquid bodies break into multiple droplets when $\psi_p > 1$, with more droplets generated at larger ψ_p. Three distinct breakup types are seen. For type **3**, a tiny satellite droplet appears after the breakup of the liquid thread at the bottom, shown by the arrow in Fig. 4(c). When ψ_p increases, type **4** is observed where the liquid thread breaks into three droplets with two large ones at the

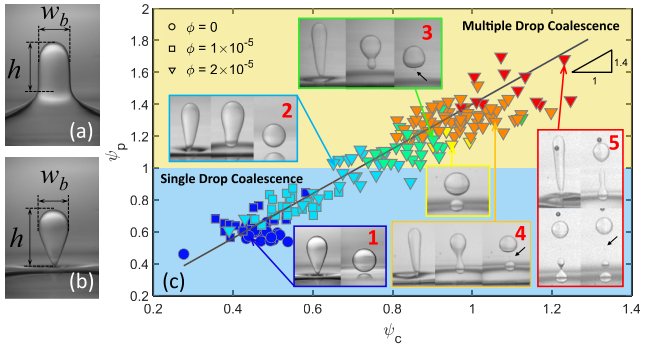

FIG. 4. Shapes of the liquid body at (a) the cylinder generation and (b) the pinch-off. (c) The breakup of the thin liquid bodies in a ψ_p-ψ_c map. The symbols are plotted in color to distinguish the 5 types of breakups as shown in the insets. The dark line represents a fitting law of $\psi_p = 1.4\psi_c$.

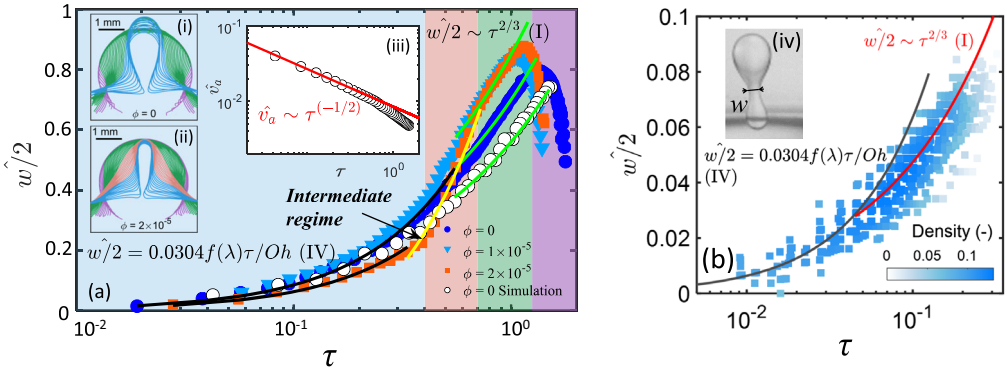

FIG. 5. (a) Neck width evolution during the pinch-off of the mother drop. Half of the neck width, $\widehat{w/2}$, is used for comparison with previous studies. The shades in purple, green, pink, and light blue roughly depict the expansion, inertial, intermediate and inertial-viscous regimes. The green lines refer to the law of $\hat{w} \sim \tau^{2/3}$ and the black lines are for $\widehat{w/2} = 0.0304\lambda^{1.46}\tau/\mathrm{Oh}$. The yellow line is plotted to show the intermediate regime. The insets (i) and (ii) illustrate the drop surface evolution with colours corresponding to each regime. (iii) Presents the change of maximum axial velocity $\widehat{v_a}$ in the simulation for $\phi = 0$. (b) Neck width evolution during the breakup of liquid threads for over 30 events for coalescence types **3**, **4** and **5**. The inset (iv) depicts how the neck width is measured.

top and the bottom, and a smaller one in the middle. Among the events in type **4**, a subtype is also captured as shown in yellow box in Fig. 4(c), where the liquid thread is too short to produce the middle satellite droplet. Type **5** is established when $\psi_p > 1.4$ where four droplets form.

To compare the dynamics of the pinch-off of mother droplets and the subsequent breakup of the liquid threads, the evolution of neck width $\hat{w}$, normalized by the radius of the mother droplet R, is tracked during the process. The tracking time is $\tau = (t_p - t)/t_\sigma$, where t_p is the instant where pinch-off occurs. For both experiments and simulations for the mother drop at $\phi = 0$, $\hat{w}$ starts to decrease after an initial expansion at a law of $\hat{w} \sim \tau^{2/3}$ until $\tau \approx 0.5$ where the liquid cylinder is generated. After that, the thinning shifts to a new regime, as shown in Fig. 5(a). This agrees well with the features of the breakup of liquid filaments, where the neck thins in the inertial (I) regime at first, it may shift to the viscous (V) regime and ends in the inertial-viscous (IV) regime [29–34]. As the Ohnesorge number $\mathrm{Oh} \ll 1$, it is highly unlikely that the pinching will be in the V regime, according to Castrejón-Pita *et al.* [35]. It is found also that the dimensionless maximum axial velocity near the neck, $\widehat{v_a} = \mu_d v_a/\sigma$ in the simulation for $\phi = 0$ follows the scaling law $\widehat{v_a} \sim \tau^{(-1/2)}$ as shown in the inset (iii) in Fig. 5(a), which further confirms that pinching shifts to the IV regime [32]. In the IV regime, the scaling law of $\widehat{w/2} = 0.0304\lambda^{1.46}\tau/Oh$ applies to the neck thinning process. The viscosity ratio $\lambda = \mu_d/\mu_s$ is introduced to include the effect of the external viscosity μ_s [32,36]. The simulated neck thinning for $\phi = 0$ in Fig. 5(a) is found to converge to the same scaling law in the IV regime, even though a deviation from the experiments is seen in the I regime. This deviation is because in the simulation the droplet is considered a sphere resting on a flat interface.

The neck thinning at $\phi = 1 \times 10^{-5}$ is similar to that of $\phi = 0$, apart from a small decrease between $\tau = 0.5$ and 0.6. The decrease becomes distinct and produces an intermediate stage at $\phi = 2 \times 10^{-5}$, as shown by the yellow line in Fig. 5(a). This is also seen by Roché *et al.* [37] who argued that the surfactants accelerate the thinning of the neck. As shown in the inset (ii) of Fig. 5(a) with light pink, the sides of the droplet surface become flat in the intermediate regime, which is not seen at $\phi = 0$.

Figure 5(b) presents the neck thinning during the breakup of the liquid threads among coalescence types **3**, **4**, and **5**. Initially at around $\tau > 0.05$, the neck thins in the I regime where $\hat{w} = 0.45\tau^{2/3}$. It then shifts to the IV regime with the same law $\widehat{w/2} = 0.0304\lambda^{1.46}\tau/\mathrm{Oh}$ as that of the thinning of the main neck. These findings clearly show the similarity of the thinning during the pinch-off of mother droplets and the breakup of the daughter liquid threads.

In summary, our simulations reveal that the convergence of the capillary waves does not lead to partial coalescence directly, but helps the generation of a liquid cylinder from the mother drop. The Rayleigh-Plateau instability is found to dominate the cylinder pinch-off leading to partial coalescence. Multiple droplets can be generated after the pinch-off of the liquid bodies at $\psi_p > 1$. For both the pinch-off of mother droplets and the subsequent breakup of the liquid threads, the neck thins in the inertial (I) regime first and then the inertial-viscous (IV) regime, which agrees well with the pinching features of liquid jets due to the RP instability in previous studies [29,30,33,34,38]. At larger surfactant concentrations, an intermediate regime appears during which the cylinder thins faster. The discovery in the current work is expected to provide a new perspective for the investigation of the second-stage partial coalescence [13,24],

coalescence with surface tension gradients [39–41], and will facilitate the comparison of partial coalescence between droplets and bubbles [20].

The authors acknowledge the support from the EPSRC MEMPHIS project. Teng Dong would also like to thank the Chinese Scholarship Council (CSC) for providing his studentship. We would like to thank Qianyi Chen from TU Delft for useful suggestions on the simulation.

*Corresponding author: p.angeli@ucl.ac.uk

[1] S. T. Thoroddsen and K. Takehara, The coalescence cascade of a drop, Phys. Fluids **12**, 1265 (2000).
[2] X.-Y. Li, A. Brandenburg, G. Svensson, N. E. Haugen, B. Mehlig, and I. Rogachevskii, Condensational and collisional growth of cloud droplets in a turbulent environment, J. Atmos. Sci. **77**, 337 (2020).
[3] L. Deike, Mass transfer at the ocean-atmosphere interface: The role of wave breaking, droplets, and bubbles, Annu. Rev. Fluid Mech. **54**, 191 (2022).
[4] T. Dong, F. Wang, W. H. Weheliye, and P. Angeli, Surfing of drops on moving liquid-liquid interfaces, J. Fluid Mech. **892** (2020).
[5] R. Zhang, Y. Li, A. L. Zhang, Y. Wang, and M. J. Molina, Identifying airborne transmission as the dominant route for the spread of COVID-19, Proc. Natl. Acad. Sci. U.S.A. **117**, 14857 (2020).
[6] H.-H. Chiu, Advances and challenges in droplet and spray combustion. I. Toward a unified theory of droplet aerothermochemistry, Prog. Energy Combust. Sci. **26**, 381 (2000).
[7] A. C. Ihnen, A. M. Petrock, T. Chou, B. E. Fuchs, and W. Y. Lee, Organic nanocomposite structure tailored by controlling droplet coalescence during inkjet printing, ACS Appl. Mater. Interfaces **4**, 4691 (2012).
[8] J. B. Boreyko and C.-H. Chen, Self-Propelled Dropwise Condensate on Superhydrophobic Surfaces, Phys. Rev. Lett. **103**, 184501 (2009).
[9] G. E. Charles and S. G. Mason, The mechanism of partial coalescence of liquid drops at liquid/liquid interfaces, J. Colloid Sci. **15**, 105 (1960).
[10] L. Rayleigh, On the stability, or instability, of certain fluid motions, Proc. London Math. Soc. **1**, 57 (1879).
[11] S. Tomotika, On the instability of a cylindrical thread of a viscous liquid surrounded by another viscous fluid, Proc. R. Soc. A **150**, 322 (1935).
[12] F. Blanchette and T. P. Bigioni, Partial coalescence of drops at liquid interfaces, Nat. Phys. **2**, 254 (2006).
[13] H. Ding, E. Li, F. Zhang, Y. Sui, P. D. Spelt, and S. T. Thoroddsen, Propagation of capillary waves and ejection of small droplets in rapid droplet spreading, J. Fluid Mech. **697**, 92 (2012).
[14] H. Aryafar and H. Kavehpour, Drop coalescence through planar surfaces, Phys. Fluids **18**, 072105 (2006).
[15] F. Zhang, M.-J. Thoraval, S. T. Thoroddsen, and P. Taborek, Partial coalescence from bubbles to drops, J. Fluid Mech. **782**, 209 (2015).
[16] P. Yue, C. Zhou, and J. J. Feng, A computational study of the coalescence between a drop and an interface in Newtonian and viscoelastic fluids, Phys. Fluids **18**, 102102 (2006).
[17] X. Chen, S. Mandre, and J. J. Feng, Partial coalescence between a drop and a liquid-liquid interface, Phys. Fluids **18**, 051705 (2006).
[18] T. Dong, W. H. Weheliye, P. Chausset, and P. Angeli, An experimental study on the drop/interface partial coalescence with surfactants, Phys. Fluids **29**, 102101 (2017).
[19] T. Gilet, K. Mulleners, J.-P. Lecomte, N. Vandewalle, and S. Dorbolo, Critical parameters for the partial coalescence of a droplet, Phys. Rev. E **75**, 036303 (2007).
[20] G. Pucci, D. M. Harris, and J. W. Bush, Partial coalescence of soap bubbles, Phys. Fluids **27**, 061704 (2015).
[21] H. P. Kavehpour, Coalescence of drops, Annu. Rev. Fluid Mech. **47**, 245 (2015).
[22] See Supplemental Material at http://link.aps.org/supplemental/10.1103/PhysRevLett.131.104001 that presents the methodology of the experiments and the simulations, which include Refs. [12,17–19,23–25]; videos that display the typical partial coalescence phenomena are included as well.
[23] T. Dong, W. H. Weheliye, and P. Angeli, Laser induced fluorescence studies on the distribution of surfactants during drop/interface coalescence, Phys. Fluids **31**, 012106 (2019).
[24] F. H. Zhang, E. Q. Li, and S. T. Thoroddsen, Satellite Formation During Coalescence of Unequal Size Drops, Phys. Rev. Lett. **102**, 104502 (2009).
[25] F. Blanchette, L. Messio, and J. W. Bush, The influence of surface tension gradients on drop coalescence, Phys. Fluids **21**, 072107 (2009).
[26] A. A. Alhareth and S. T. Thoroddsen, Partial coalescence of a drop on a larger-viscosity pool, Phys. Fluids **32**, 122115 (2020).
[27] J. Hoepffner and G. Paré, Recoil of a liquid filament: Escape from pinch-off through creation of a vortex ring, J. Fluid Mech. **734**, 183 (2013).
[28] A. A. Castrejón-Pita, J. R. Castrejón-Pita, and I. M. Hutchings, Breakup of Liquid Filaments, Phys. Rev. Lett. **108**, 074506 (2012).
[29] D. T. Papageorgiou, On the breakup of viscous liquid threads, Phys. Fluids **7**, 1529 (1995).
[30] K.-L. Huang, K.-L. Pan, and C. Josserand, Pinching Dynamics and Satellite Droplet Formation in Symmetrical Droplet Collisions, Phys. Rev. Lett. **123**, 234502 (2019).
[31] R. F. Day, E. J. Hinch, and J. R. Lister, Self-Similar Capillary Pinchoff of an Inviscid Fluid, Phys. Rev. Lett. **80**, 704 (1998).
[32] J. R. Lister and H. A. Stone, Capillary breakup of a viscous thread surrounded by another viscous fluid, Phys. Fluids **10**, 2758 (1998).
[33] A. U. Chen, P. K. Notz, and O. A. Basaran, Computational and Experimental Analysis of Pinch-Off and Scaling, Phys. Rev. Lett. **88**, 174501 (2002).
[34] J. Eggers, Universal Pinching of 3D Axisymmetric Free-Surface Flow, Phys. Rev. Lett. **71**, 3458 (1993).
[35] J. R. Castrejón-Pita, A. A. Castrejón-Pita, S. S. Thete, K. Sambath, I. M. Hutchings, J. Hinch, J. R. Lister, and O. A. Basaran, Plethora of transitions during breakup of

liquid filaments, Proc. Natl. Acad. Sci. U.S.A. **112**, 4582 (2015).

[36] I. Cohen, M. P. Brenner, J. Eggers, and S. R. Nagel, Two Fluid Drop Snap-Off Problem: Experiments and Theory, Phys. Rev. Lett. **83**, 1147 (1999).

[37] M. Roché, M. Aytouna, D. Bonn, and H. Kellay, Effect of Surface Tension Variations on the Pinch-Off Behavior of Small Fluid Drops in the Presence of Surfactants, Phys. Rev. Lett. **103**, 264501 (2009).

[38] M. P. Brenner, J. R. Lister, and H. A. Stone, Pinching threads, singularities and the number 0.0304..., Phys. Fluids **8**, 2827 (1996).

[39] C. Constante-Amores, A. Batchvarov, L. Kahouadji, S. Shin, J. Chergui, D. Juric, and O. Matar, Role of surfactant-induced Marangoni stresses in drop-interface coalescence, J. Fluid Mech. **925** (2021).

[40] K. Sun, P. Zhang, Z. Che, and T. Wang, Marangoni-flow-induced partial coalescence of a droplet on a liquid/air interface, Phys. Rev. Fluids **3**, 023602 (2018).

[41] M. A. Hack, P. Vondeling, M. Cornelissen, D. Lohse, J. H. Snoeijer, C. Diddens, and T. Segers, Asymmetric coalescence of two droplets with different surface tensions is caused by capillary waves, Phys. Rev. Fluids **6**, 104002 (2021).